Copoly(imide siloxane) Abhesive Materials with Varied Siloxane Oligomer Length

C.J. Wohl[1], B.M. Atkins[2], Y. Lin[3], M.A. Belcher[3], J.W. Connell[1], NASA Langley Research Center, Hampton, VA 23681-2199, United States[1],Langley Aerospace Research Summer Scholars (LARSS), NASA Langley Research Center, Hampton, VA 23681-2199, United States[2], National Institute of Aerospace, Hampton, VA, 23666-6147, United States[3]

Email: christopher.j.wohl@nasa.gov

Introduction

High fidelity surface engineering involves both chemical and topographical modifications and is emerging as a promising way to adapt materials for highly specialized applications. For example, polydimethyl siloxane (PDMS) surfaces can be engineered to exhibit various geometric configurations in response to strain, and varying degrees of wettability as a result of controlled chemical modification [1]. Surface engineered materials are used for purposes such as anti-icing, mitigation of surface contamination in microelectronics fabrication, biofouling in marine environments, mitigation of biofilm formation, and extra-terrestrial exploration applications. To this end, surface engineering of polyimides was investigated as a method to generate abhesive (non-stick) materials. Polyimides have been used extensively, due to superior properties, such as low moisture uptake, good electrical insulating properties, excellent thermal stability, good mechanical properties, and have a long history as a space-qualified material [2]. Copoly(imide siloxane)s have demonstrated greater utility in specific applications by pairing the polyimide material properties with those of the siloxane portion. This results in; better processability, increased impact resistance, decreased dielectric constants [3], and of greatest significance for this work, a reduction of the material's surface energy [4].

In this work, copoly(imide siloxane) materials were investigated for abhesive applications. The surface energy of a material, γ, plays a pivotal role in determining the material's wettability, adhesive capability, propensity for particulate adhesion, and chemical resistance. Materials with high surface energies are more easily wetted by incident solvents, capable of greater adhesive bond strength with other substrates, and more likely to accumulate surface contaminants (both chemical contamination and debris). Therefore, the generation of low surface energy materials is important for environments where debris free non-adhesive surfaces are of paramount importance. NASA's return to lunar exploration presents another application for low surface energy abhesive materials as lunar dust poses major challenges to mission success [5]. Lunar dust is classified as the portion of the surface regolith ranging in size from 50 μm and lower and is comprised of a diverse collection of mineralogical compositions. These particles are abrasive, highly porous, electrostatically charged, chemically activated, and can be magnetic [6-10]. There is also evidence that lunar dust has a dynamic component with the greatest degree of mobility occurring at the terminator - the separation between day and night sides of the lunar surface - due to the dramatic change in electrostatic potential present there [11, 12]. With these properties, lunar dust presents a tremendous challenge for the successful completion of both manned and robotic lunar missions. A materials-based approach to mitigate the lunar dust hazard requires modification of a material's surface properties. To this end, low surface energy copoly(imide siloxane)s were generated with various siloxane segment lengths. The migration of the siloxane oligomers to the surface was characterized using contact angle goniometry and the adhesion of various particulates to the copoly(imide siloxane)s films was investigated using a sonication device.

Experimental

Materials

Prior to use, 2,2-bis(3,4-dicarboxyphenyl)hexafluoropropane dianhydride (6FDA, Clariant Corporation, T_m = 242 °C) was vacuum dried. 4,4'-oxydianiline (4,4'-ODA, Wakayama Seika Kogya Co. Ltd, T_m=188 °C) and aminopropyl-terminated siloxanes (Gelest) were used as received. ^{1}H NMR spectra were recorded on a Bruker instrument operating at 300.152 MHz. The number average molecular weight of the siloxane materials was determined using ^{1}H NMR spectroscopy by calculating the ratio of methylene protons of the aminopropyl groups to the methyl groups on the siloxane repeat units. In some cases, the experimentally determined molecular weight differed from the manufacturer's values (Table 1). Differential scanning calorimetry (DSC) was conducted using a Setaram Instrumentation DSC 131 with a heating rate of 20 °C/min. Polymer film mechanical properties were determined on a Sintech 2W with a crosshead speed of 5.08 mm/min according to ASTM D882. The data were collected and analyzed using Testworks 8.0. Material surfaces were imaged using a Zeiss LSM 5 Exciter confocal microscope and an Olympus BH-2 optical microscope equipped with a Hitachi KP-D50 digital color camera. Water contact angle data were collected using a First Ten Angstroms FTA 1000B contact angle goniometer. Tilting axis contact angles were measured for each sample using an 8 μL water droplet. Interfacial tension measurements of a suspended water drop were made prior to experimentation to verify water purity and precision of the focused image. Contact angles were determined by drop shape analysis from a series of images collected at a rate of 2 frames/s. The stage of the contact angle instrument was tilted at a rate of 2 °/s to an inclination of 60°. A minimum of two measurements was recorded for each sample.

Table 1. Molecular weights for the siloxane materials.

Siloxane	Designation	Molecular Weight (g mol^{-1}) Reported	^{1}H NMR Analysis*	Number of repeat units
Disiloxane	S1	249	249	1
DMS-A11	S2	875	1150	12
DMS-A15	S3	3000	2980	37
DMS-A21	S4	5000	6150	80
DMS-A32	S5	30000	35800	480

*[13]

Polymer synthesis

Polyimides were prepared by the condensation reaction of stoichiometrically equivalent amounts of 6FDA and 4,4'-ODA (**Scheme 1**). The reaction vessel was flushed with nitrogen for 10 minutes prior to the addition of any reactants. Reactions were carried out under nitrogen at 20 wt. % solids in *N*-methylpyrrolidinone (NMP). The diamine was dissolved in NMP, to which the dianhydride was added, followed by additional NMP to achieve the desired concentration, typically 10-20% solids. The reaction mixture was mechanically stirred overnight.

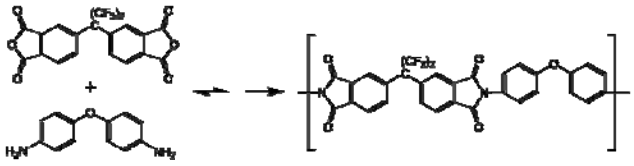

Scheme 1: Polyimide synthesis.

Copoly(imide siloxane)s were similarly prepared using a solvent mixture of 4:1 NMP and tetrahydrofuran (THF). The PDMS component (10 wt. % of the total solids) was dissolved in THF and added to the reaction vessel at the same time as the 4,4'-ODA (a representative structure is shown in **Scheme 2**). For brevity, the names of the copoly(imide siloxane)s generated here have been assigned designations corresponding to their monomeric composition. The designations for the siloxane component can be found in **Table 1** and the definition of the different polyimide monomeric compositions can be found in **Table 2**. For example, a polymer synthesized from 6FDA and 4,4'-ODA without the addition of a siloxane component would be assigned the designation PIS0, while a polymer comprised of the same two monomers with the addition of the PDMS with a molecular weight of 2980 g mol^{-1} would be labeled as PIS3. Inherent viscosities (η_{inh}) were determined at 25 °C on amide acid solutions using an Ubbelohde viscometer and solution concentrations of 0.5 g dL^{-1} (**Table 2**). Films were cast on glass plates or polished stainless steel using a doctor blade and placed in a forced air drying chamber until "tack-free." Films were

thermally imidized under nitrogen using a cure cycle with stages at 150, 175, 200, and 250 °C with at least a 40 min hold at each temperature.

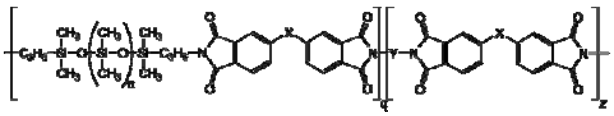

Scheme 2: Copoly(imide siloxane) structure. X is the hexafluoropropyl portion of 6FDA and Y is the diphenyl ether portion of 4,4'-ODA.

Table 2. Copoly(imide siloxane) designations and inherent viscosity values. For dianhydride and diamine structures, refer to Scheme 1.

Copolymer Designation	Siloxane Oligomer	η_{inh}, dL g^{-1}	Film Opacity
PIS0	None	1.42	Transparent
PIS1	Disiloxane	0.21	Transparent
PIS2	DMS-A11	0.91	Transparent
PIS3	DMS-A15	0.95	Opaque
PIS4	DMS-A21	1.28	Opaque
PIS5	DMS-A32	1.14	Opaque

Laser Ablation Patterning

A 0°/90° crosshatch pattern was etched onto polymer film surfaces (1 cm^2) using a PhotoMachining, Inc. laser ablation system equipped with a Coherent Avia® frequency-tripled Nd:YAG laser (λ = 355nm, 7 W). The laser beam pulse energy, diameter, and scan speed were kept constant at 66.2 μJ pulse^{-1}, 25 μm and 25.4 cm/s, respectively. Line spacing was maintained at 25 μm.

Adhesion Testing

Particle adhesion testing was performed using an in-house device modeled after a similar instrument described in the literature [14, 15]. A polymer film sample was attached to the end of a sonic wand tip (VCX-750, Sonics and Materials, Inc.). Lunar dust simulant (NASA/USGS Lunar Highland simulant, maximum particle diameter <30 μm) was deposited on the polymer surface by placing the polymer film in a plastic bag containing the simulant. Agitation of the bag caused simulant to become airborne and deposit on the film surface. The sonic wand was then suspended over a laser optical particle counter (Solair 3100, Lighthouse Worldwide Solutions) in a horizontal configuration, with the entire assembly housed in an environmental chamber (Abbess Instruments). By varying the sonic wand's vibrational amplitude, particles were dislodged from the polymer film and fell into the optical particle counter where size distribution was determined. Adhesion force values were calculated according to the size of the particles detected in the optical particle counter. After the adhesion testing was completed, the film samples were removed from the device assembly and observed by optical microscopy to identify the particles still adhered to the surface. For the surfaces investigated here, particles remaining on the surface had lower calculated boundary adhesion force values.

Results and Discussion

Polymer synthesis and characterization

Copoly(imide siloxane)s were synthesized to generate low surface energy materials for abhesive applications. The siloxane oligomer length was varied to investigate the domain formation/phase segregation and surface migration behavior of the siloxane moieties as a function of siloxane size. Within a given concentration (i.e. 10% siloxane), the incorporation of smaller siloxane moieties was found to preserve the transparency of the copolymer film, while incorporation of siloxane oligomers 2980 g mol^{-1} or higher resulted in an opaque film, suggesting that the copolymer was phase segregated (**Table 2**). Phase segregation in similar copolymers was observed using electron microscopy and small angle neutron scattering to visualize the segregated domains [16]. Further evidence for this was observed in the thermal and mechanical analyses of these materials.

The thermal properties of a material often provide insight into the chemical structure and long range ordering within the bulk material. DSC was used to understand how the incorporation of siloxane oligomers affected these properties within a polyimide matrix. T_g values varied significantly depending on the length of siloxane oligomer present in the copoly(imide siloxane). Smaller siloxane moieties resulted in dramatic reductions in T_g values, while larger siloxane components resulted in less dramatic changes (**Figure 1A**). This is further evidence that the larger siloxane oligomers exhibited greater phase separation within the polyimide matrix, which is in agreement with the differences in film transparency. The change in heat capacity for a series of copoly(styrene siloxane) materials indicated that the degree of phase mixing (**DPM)** was dependent on siloxane segment lengths (with larger segment lengths exhibiting lower DPM values) similar to the results presented here [17]. If the two polymers were miscible, the addition of siloxanes should reduce the T_g according to the Fox equation (which relates a copolymer's T_g to the relative weight percentages and T_g for each homopolymer). Although the weight percent of the siloxane containing polyimide portion should be lower, since the number of amine functionalities for the larger siloxanes is less, the difference in the calculated T_g values does not correlate with the data collected for these materials. Phase transitions arising from the siloxane moieties themselves would not have been observable in the experiments conducted here because their T_g values are well below room temperature (typically < -120 °C).

The addition of siloxane moieties also resulted in a decrease in the Young's modulus compared to the 6FDA:4,4'-ODA homopolyimide (**Figure 1B**) with larger siloxane functionalities resulting in greater reductions in modulus. This may be due to increased disruption of the polyimide domains (the major contributor to the modulus). The trend observed in this data suggests that a minimum modulus value (approximately 75% of the homopolyimide value) was obtained upon increasing the siloxane molecular weight to 2980 g mol^{-1}.

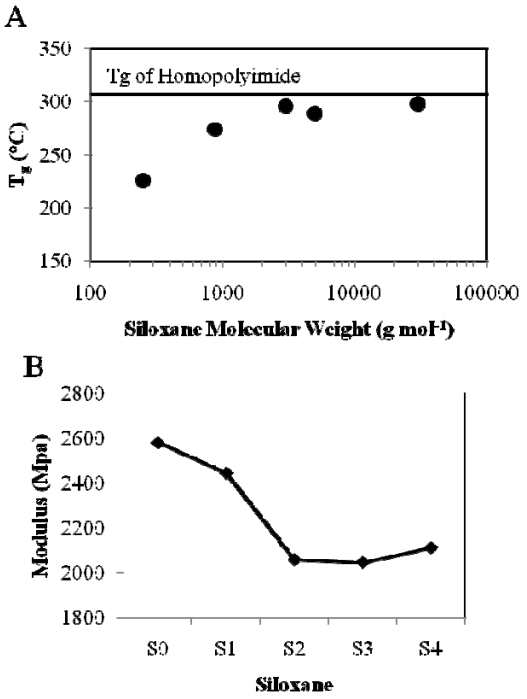

Figure 1. (A) T_g values for the copoly(imide siloxane)s. T_g value for the homopolyimide, 307 °C. (B) The modulus decreased with increased siloxane molecular weight.

Contact Angle Analysis

The surface energy of a material is one of several indicators of the likelihood for adhesive interaction with contaminants through non-mechanical interactions (chemical vs. physical attachment). Here, surfaces with lower surface energies would be anticipated to exhibit reduced adhesive interactions. The surface energy of a material was determined by measuring the contact angle that solvents of known surface tension make with the interrogated surface. Higher contact

angle values correlate with lower surface energies. Water contact angles were collected from images of 8 μL drops deposited on the copolymer film surfaces, which were subsequently subjected to tilting angles up to 60° (**Figure 2**). Advancing water contact angle values, θ_{adv}, indicated that increased siloxane molecular weight resulted in greater θ_{adv} values. Copoly(imide siloxane)s generated with the S5 siloxane (Mw = 35,800 g mol^{-1}) exhibited the greatest θ_{adv} values approaching that of Teflon® (θ_{adv} ~ 110°). This increase in θ_{adv} values suggests a high population of the siloxane moieties on the polymer surface. The data also suggested that θ_{adv} could increase further via incorporation of larger siloxane moieties. However, this is unlikely as the equilibration between the gravitational forces causing the water droplet to spread and cohesive forces causing the water droplet to retain a spherical shape are balanced. Thus, regardless of interfacial interactions, gravitational forces will supersede cohesive forces on a topographically smooth surface, resulting in a θ_{adv} value ≤ 120°. A further reduction in surface energy required a reduction in the interaction area that was achieved via topographical modification as described below.

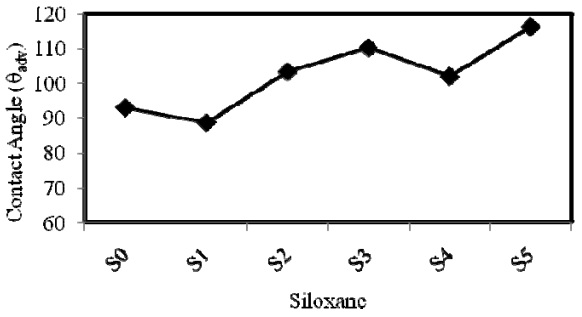

Figure 2. Contact angle data for copoly(imide siloxane) materials. Increasing the molecular weight of the siloxane moiety resulted in increased θ_{adv} values.

Laser Ablation Patterning

As the contact angles θ_{adv} indicated (**Figure 2**), generation of copoly(imide siloxane) materials greatly reduced the material's surface energy and implicitly, the propensity of particulate contamination. To further increase θ_{adv} values and reduce the surface energy, the surfaces were topographically modified using laser ablation patterning. Laser patterning affords a precise, high-fidelity process with several adjustable parameters enabling transcription of a variety of patterns and variation thereof. In previous work, a series of experiments was performed to determine the appropriate laser parameters to impart topographies on the copolymer film surfaces [18]. The settings necessary to generate topographical features several microns in height were determined to be 5.25 W laser pulses with a frequency of 80 kHz (resulting in 66.2 μJ per pulse) and a scan speed of 25.4 cm s^{-1}. Highly accurate sample alignment enabled several transcription steps to be performed on a sample surface with nearly exact overlap of previous steps. This approach was adopted to transcribe 0°/90° crosshatch patterns, four times to increase the ablation depth, onto copoly(imide siloxane) films covering an area of several square centimeters. Optical and confocal micrographs verified the fidelity of this process over large length scales (data not shown)

The introduction of topographies increased the water θ_{adv} values for all materials investigated here. **Figure 3** provides an example of the increase in θ_{adv} values for 6FDA:4,4'-ODA homopolyimide (PIS0, top) and a copoly(imide siloxane) (PIS4, bottom). The increase in θ_{adv} was greater for the copolymeric materials than for the homopolyimide surfaces, except for copolymers that incorporated the S1 siloxane. Contact angle θ_{adv} values determined for laser ablation patterned surfaces approached 180°C and were classified as superhydrophobic ($\theta_{adv} \geq 150°$). Roll-off angles are further indications of the propensity of particles to adhere to surfaces, with a low roll-off angle indicating the incident solvent does not wet the surface. If a material exhibits a shallow roll off angle, presumably a shallow tilting angle would be required to remove contaminating particles. Although large θ_{adv} values are indicative of low surface energies, there are examples in the literature where water droplets strongly adhered to a superhydrophobic surface [19]. Roll-off angles for several laser ablation patterned copoly(imide siloxane)s were < 10°, with values as low as 2° observed, suggesting that laser ablation patterned copoly(imide siloxane) surfaces should exhibit greater mitigation capabilities of particulate adhesion compared to non-patterned surfaces (data not shown).

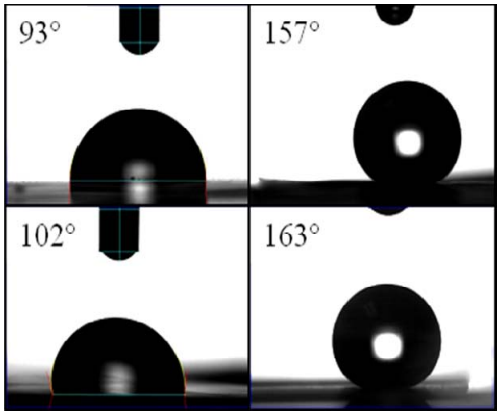

Figure 3. Images of water drops used to determine contact angles observed on PIS0 [top, homopolyimide] and PIS4 [bottom, copoly(imide siloxane)] before (left) and after (right) laser ablation patterning.

Particle Adhesion Testing

A more direct method to evaluate the efficacy of the copoly(imide siloxane) materials for abhesive applications was to test particulate adhesion. To do this, a device was constructed to measure the retention of particulate matter on an intentionally contaminated surface (113 mm^2) after the application of external stimulus [14]. The external stimulus was provided by sonication of a sample affixed to the end of a sonic wand. Activation of the sonic wand induced vibration at the tip that resulted in an acceleration force acting normal to the sample plane, F_{sw}, determined by the acceleration of the tip, a, the frequency of oscillation, ω, and the amplitude of displacement, A. Adhered particles were dislodged from the surface when the sonic wand acceleration force, F_{sw}, exceeded the adhesion force, F_{adh} (**Eq. 1**),

$$F_{sw} = ma = m(4\pi^2\omega^2 A) > F_{adh} \quad [1]$$

where m is the dislodged particle's mass. The particles were assumed to be spherical with a density of 2.9 g cm^{-3}. A protocol was established to test the adhesion force of particles to a sample surface by variation of sonic wand amplitude from 20 – 80 % corresponding to surface acceleration values from 380 – 1550 km s^{-2}. Dislodged particles were collected and sized in a laser optical particle counter. The size of these particles was then used to calculate an adhesion force based on the amplitude setting of the sonic wand. For comparison purposes, a commercially available polyimide (Kapton® HN) was tested along with **PIS4** and a laser ablation patterned **PIS4** surface. The samples were affixed to the sonic wand tip using an acrylic adhesive and coated with lunar simulant. After completion of the sonic wand amplitude protocol, each sample demonstrated retention of particulate matter (i.e., $F_{adh} \geq F_{sw}$, **Figure 4**). The size of particles on the surface was determined using optical microscopy, and a lower bound for the adhesion force was calculated. The particle count and adhesion force for each surface are indicated in **Table 3**. The copoly(imide siloxane) material had a demonstrated decrease in both particle count and adhesion force relative to Kapton® HN. Laser ablation patterning further reduced the number of adhered particles and the adhesion force.

Figure 4. Sonic wand adhesion testing indicated that the polyimide surface (A) retained a greater number of particles than the copoly(imide siloxane) surface both before (B) and after laser ablation patterning (C). The lunar simulant particle retained on the laser ablation patterned surface can be seen near the center of the image. The scale bar is 25 μm.

Table 3. Preliminary adhesion testing results.

Material	Particles Remaining in 113 mm^2 area	Adhesion Force, nN
Kapton® HN	~378	156
PIS4	~252	112
Laser Patterned PIS4	1 - 2	10 - 68

Conclusions

In this work, low surface energy copoly(imide siloxane)s were synthesized with various siloxane segment lengths. Characterization of these materials revealed that domain formation of the low surface energy component within the matrix was more prevalent for longer siloxane segments as indicated by increased opacity, decreased mechanical properties, and variation of the T_g. Incorporation of siloxanes lowered the polymer's surface energy as indicated by water contact angle values. Topographical modification of these materials by laser ablation patterning further reduced the surface energy, even generating superhydrophobic surfaces.

Combined, the contact angle data and particle adhesion testing indicated that copoly(imide siloxane) materials may provide greater mitigation to particulate adhesion than polyimide materials alone. These enhanced surface properties for abhesive applications did result in a reduction of the tensile moduli of the copolymers. It is possible that lower siloxane loading levels would result in retention of the mechanical properties of the polyimide while still affording abhesive surface properties. This hypothesis is currently being investigated. Laser ablation patterning offers further reduction in particle retention as the available surface area for particle adhesion is reduced. Pattern variation and size dependencies are currently being evaluated.

For the purposes of lunar dust adhesion mitigation, it is likely that this approach, termed passive due to the lack of input from an external energy source, would not be sufficient to mitigate surface contamination or clean contaminated surfaces for some lunar applications. It is feasible to combine these materials with active mitigation strategies - methods that utilize input from external energy sources - would broaden the applicability of such materials for abhesive purposes. Collaborative efforts along these lines have been initiated with researchers at NASA Kennedy Space Center where experiments are being conducted involving a series of embedded electrodes within polymeric matrices.[20]

Acknowledgements

The authors would like to thank Professor Michael E. Mullins, Michigan Technological University, for discussions concerning the manufacture of the particle adhesion testing device and Dr. Jeffrey A. Hinkley, NASA Langley Research Center, for scientific discussion. This work was funded through the NASA Langley Research Center's Creative and Innovative Research Fund.

References

1. Crowe, J.; Efimenko, K.; Genzer, J., Manipulating Siloxane Surfaces: Obtaining the Desired Surface Function via Engineering Design. In *Science and Technology of Silicones and Silicone-Modified Materials.*, Clarson, F.; Fitzgerald, J.; Owen, M.; Smith, S.; Van Dyke, M., Eds. American Chemical Society: 2007; p 384.

2. *Polyimides*. Wilson, D.; Stenzenberger, H. D.; Hergenrother, P. M., Eds.; Chapman and Hall: New York, 1990; p 297.

3. Mahoney, C. M.; Gardella, J. A.; Rosenfeld, J. C., *Macromolecules* **2002,** 35, 5256.

4. Park, H. B.; Han, D. W.; Lee, Y. M., *Chem. Mater.* **2003,** 15, 2346.

5. Taylor, L. A.; Schmitt, H. H.; Carrier, W. D.; Nakagawa, M., The Lunar Dust Problem: From Liability to Asset. In *1st Space Exploration Conference: Continuing the Voyage of Discovery*, American Institute of Aeronautics and Astronautics: Orlando, Florida, 2005.

6. Colwell, J. E.; Batiste, S.; Horanyi, M.; Robertson, S.; Sture, S., *Rev. Geophys.* **2007,** 45, 2005RG000184.

7. Abbas, M.; Tankosic, D.; Craven, P.; Spann, F.; LeClair, A.; West, E., *Planet. Space Sci.* **2007,** 55, 953.

8. Halekas, J.; Lin, R.; Mitchell, D., *Geophys. Res. Lett.* **2007,** 32, L09102.

9. Sternovsky, Z.; Sickafoose, A. A.; Colwell, J. E.; Robertson, S.; Horanyi, M., *J. Geophys. Res.* **2002,** 107, 15-1.

10. Taylor, L. A.; Meek, T. T., *J. Aerospace Eng.* **2005,** 18, 188.

11. Borisov, N.; Mall, U., *Planet. Space Sci.* **2006,** 54, 572.

12. Stubbs, T.; Vondrak, R.; Farrell, W., *Adv. Space Res.* **2006,** 37, 59.

13. Hatada, K.; Kitayama, T., *NMR Spectroscopy of Polymers*. Eds.; Springer Verlag: Berlin, Germany, 2004.

14. Mullins, M.; Micheals, L.; Menon, V.; Locke, B.; Ranade, M., *Aerosol Sci. Technol.* **1992,** 17, 105.

15. Zimon, A., *Adhesion of Dust and Powder*. Corn, M., Eds.; Plenum Press: New York, 1969.

16. Samseth, J.; Mortensen, K.; Burns, J. L.; Spontak, R. J., *J. Appl. Polym. Sci.* **1992,** 44, 1245.

17. Feng, D.; Wilkes, G. L.; Crivello, J. V., *Polymer* **1989,** 30.

18. Wohl, C. J.; Belcher, M. A.; Chen, L.; Connell, J. W., *Langmuir* **2010,** 26, 11469.

19. Winkleman, A.; Gotesmann, G.; Yoffe, A.; Naaman, R., *Nanoletters* **2008,** 8, 1241.

20. Immer, C.; Starnes, J.; Michalenko, M.; Calle, C.; Mazumder, M., Electrostatic Screen for Transport of Martian and Lunar Regolith. In *37th Lunar and Planetary Science Conference*, Lunar Planetary Institute: League City, Texas, 2006; Vol. abstract # 2265.